Platelets

ISSN: (Print) (Online) Journal homepage: https://www.tandfonline.com/loi/iplt20

Comparison of the effects of platelet concentrates produced by high and low-speed centrifugation protocols on the healing of critical-size defects in rat calvaria: a microtomographic and histomorphometric study

Lucia Moitrel Pequeno da Silva, Débora de Souza Ferreira Sávio, Felipe Correa de Ávila, Raphael Martini Vicente, Gabriel Guerra David Reis, Ricardo Junior Denardi, Natacha Malu Miranda da Costa, Pedro Henrique Felix Silva, Carlos Fernando de Almeida Barros Mourão, Richard J. Miron & Michel Reis Messora

To cite this article: Lucia Moitrel Pequeno da Silva, Débora de Souza Ferreira Sávio, Felipe Correa de Ávila, Raphael Martini Vicente, Gabriel Guerra David Reis, Ricardo Junior Denardi, Natacha Malu Miranda da Costa, Pedro Henrique Felix Silva, Carlos Fernando de Almeida Barros Mourão, Richard J. Miron & Michel Reis Messora (2022): Comparison of the effects of platelet concentrates produced by high and low-speed centrifugation protocols on the healing of critical-size defects in rat calvaria: a microtomographic and histomorphometric study, Platelets, DOI: 10.1080/09537104.2022.2071851

To link to this article: https://doi.org/10.1080/09537104.2022.2071851

http://www.tandfonline.com/iplt
ISSN: 0953-7104 (print), 1369-1635 (electronic)

platelets

Platelets, Early Online: 1–10
 DOI: https://doi.org/10.1080/09537104.2022.2071851

Taylor & Francis
Taylor & Francis Group

ORIGINAL ARTICLE

Check for updates

Comparison of the effects of platelet concentrates produced by high and low-speed centrifugation protocols on the healing of critical-size defects in rat calvaria: a microtomographic and histomorphometric study

Lucia Moitrel Pequeno da Silva [1], Débora de Souza Ferreira Sávio [2], Felipe Correa de Ávila [2], Raphael Martini Vicente [3], Gabriel Guerra David Reis [1], Ricardo Junior Denardi [1], Natacha Malu Miranda da Costa [1], Pedro Henrique Felix Silva [1], Carlos Fernando de Almeida Barros Mourão [4], Richard J. Miron [5], & Michel Reis Messora [1]

[1]Department of Oral and Maxillofacial Surgery and Periodontology – DCTBMF, School of Dentistry of Ribeirão Preto, University of São Paulo, Ribeirão Preto, SP, Brazil, [2]Department of Morphology, Physiology, and Basic Pathology – DMFPB, School of Dentistry of Ribeirão Preto, University of São Paulo, Ribeirão Preto, SP, [3]Department of Orthopedics and Anesthesiology, Ribeirão Preto Medical School, University of São Paulo – USP, Ribeirão Preto, São Paulo, Brazil, [4]Clinical Research Unit, Antônio Pedro University Hospital, Fluminense Federal University, Rio de Janeiro, Brazil, and [5]Department of Periodontology, University of Bern, Bern, Switzerland

Abstract

The current study evaluated the healing of critical-size defects (CSD) created in rat calvaria treated with platelet concentrates produced by high-speed (Leukocyte- and Platelet-Rich Fibrin - L-PRF) and low-speed (Advanced Platelet-Rich Fibrin - A-PRF) protocols of centrifugation. Twenty-four rats were distributed into three groups: Control, L-PRF, and A-PRF. Five mm diameter CSD were created on the animals' calvaria. The defects of the L-PRF and A-PRF groups were filled with 0.01 ml of L-PRF and A-PRF, respectively. The control group defects were filled with a blood clot only. All animals were euthanized on the 35th postoperative day. Histomorphometric and microtomographic analyses were then performed. The L-PRF and A-PRF groups had significantly higher bone volume and neoformed bone area than those of the control group and lowered bone porosity values ($p < .05$). No significant differences were observed between A-PRF and L-PRF groups for the analyzed parameters. Therefore, it can be concluded that i) L-PRF and A-PRF potentiated the healing of CSD in rat calvaria; ii) high and low-speed centrifugation protocols did not produce PRF matrices with different biological impacts on the amount of bone neoformation.

Keywords

Blood platelet, bone regeneration, fibrin platelet-rich fibrin

History

Received 25 November 2021
Revised 16 March 2022
Accepted 12 April 2022

Introduction

In the early 2000s, Choukroun introduced the second generation of platelet concentrates terming platelet-rich fibrin (PRF)[1]. In this blood-by-product, the fibrinogen initially concentrates in the upper part of the tube until the circulating thrombin transforms it into fibrin, forming a three-dimensional fibrin clot, rich in platelets and leukocytes, which stays concentrated in this network. The original Leukocyte- and Platelet-Rich Fibrin (L-PRF) matrix was considered a natural biomaterial that includes all cells and cytokines essential for ideal healing. It also favors the microvascularization of the site and can guide epithelial cell migration to its surface. From a clinical point of view, this biomaterial accelerates physiological healing due to the presence of these molecules and its three-dimensional tetramolecular architecture [2,3].

L-PRF is used clinically in several fields of regenerative dentistry, such as post-extraction socket filling [4–8], regeneration of periapical defects [9–11], maxillary sinus lifting [12–17], treatment of gingival recessions [18–20], treatment of intraosseous periodontal defects [21,22], and even in the management of bone osteonecrosis related to the use of bisphosphonates [23,24]. The technique is considered an easy, short, low cost, and minimally invasive protocol, demonstrating promising results. In this technique, the patient's peripheral blood is collected in specific tubes without anticoagulants and immediately centrifuged for 12 minutes at 2700 rotations per minute (rpm; ~700 RCF-max)[1].

In some histological analyzes of L-PRF, it was possible to attest that most platelets were concentrated in the lower part of the matrix, close to the red cell zone, with studies demonstrating that this lower portion of the PRF matrix is clinically more important than its upper counterpart [25–28]. This distribution pattern is due to the high centrifugation speed, which "pushed" platelets and leukocytes downward [26]. However, aiming to produce the PRF matrix with a better distribution of platelets and leukocytes, the concept of "low-speed centrifugation" was created. Several new protocols emerged with this new concept in mind, including Advanced Platelet-Rich Fibrin (A-PRF)[26].

For the production of A-PRF, the technique is very similar to L-PRF. However, the centrifugation speed is reduced to 1500 rpm (~208 g) with a period of 14 minutes [26]. This results in a solid matrix that, despite being smaller than L-PRF, has a more

Correspondence: Michel Reis Messora, Department of Oral and Maxillofacial Surgery and Periodontology – DCTBMF, School of Dentistry of Ribeirão Preto, University of São Paulo, Ribeirão Preto, SP, Brazil. Email: m.messora@forp.usp.br

homogeneous distribution of leukocytes throughout its matrix [27,28]. Furthermore, more platelets and neutrophilic granulocytes are found in the distal portion of A-PRF, influencing the differentiation of host and matrix macrophages following its implantation [26]. In addition, it has a more porous structure with a larger interfibrous space than L-PRF, which significantly facilitates cell penetration into the fibrin matrix, showing a significantly greater vascularization when compared to L-PRF ten days after its subcutaneous implantation in rats [26,28–30].

Engler-Pinto et al [31]. demonstrated that L-PRF increased the amount of neoformed bone in critical-size defects (CSD) in rats with induced osteoporosis by ovariectomy and the osteoconductive potential of bovine bone grafts. However, to date, no study has evaluated whether platelet concentrates produced with lower centrifugation speeds, such as A-PRF, would be more beneficial for bone healing when compared to standard L-PRF. Therefore, the purpose of this study was to evaluate the healing of CSD created in rat calvaria and treated with L-PRF or A-PRF.

Methods

Sample

The research was conducted only after the approval of the Ethics Committee on Animal Use of the School of Dentistry of Ribeirão Preto (FORP) of the University of São Paulo (USP) (Protocol n° 2019.1.752.58.4).

A power of 80% was adopted to detect a significant difference of 20% between groups with a confidence interval of 95% ($\alpha = 0.05$) and a standard deviation of 15%[32], considering changes in the means of neoformed bone as the primary variable. Thus, a sample size of 8 animals per group was adopted.

Experimental model

Twenty-four 14-week old rats (*Rattus norvegicus albinus*, Wistar), weighing 350–450 g (Central Animal Facility, FORP-USP, Ribeirão Preto, SP, Brazil), were used. The animals were kept in a room with a 12-hr light/dark cycle and temperature between 22–24°C. They were fed with a selected solid diet and water *ad libitum*. They were randomly distributed into three experimental groups (n = 8): Control (C), L-PRF, A-PRF. All analyses were performed by calibrated and blinders examiners.

The animals were initially induced in a chamber with 4% Isoflurane (Instituto Biochimico Ind. Farm. Ltda, Itatiaia, RJ, Brazil) and kept in inhalation anesthesia by mask with the same anesthetic at 1.5–3%. After anesthetic induction, morphine sulfate (Dimorf, Cristália® Prod. Quim. Farm. Ltd., Itapira, SP, Brazil; 8 mg/kg) and penicillin G-benzathine (Pentabiótico Veterinário Pequeno Porte, Fort Dodge Animal Health®, Campinas, SP, Brasil; 24.000 UI/Kg) were administered intramuscularly. In addition, subcutaneous injection of Flunixin Meglumine (Aplonal 1%, König®, Buenos Aires, Argentina; 2 mg/kg) was also administered.

Preparation of platelet concentrates matrices

Three mL of blood from each animal were collected through a cardiac puncture, using a 5 mL disposable syringe (Descarpack®, São Paulo, SP, Brazil). The blood drawn was transferred to a 5-mL silica-coated plastic tube without additives (BD Vacutainer®, Becton, Dickinson and Company, Franklin Lakes, NJ, USA) and immediately processed to prepare L-PRF or A-PRF.

The preparation of L-PRF and A-PRF were carried out according to the protocol proposed by Choukroun et al [26]. In the L-PRF group, immediately after the blood collection, the blood was centrifuged at 2700 rpm for 12 minutes (relative centrifugal force maximum – RCF-max = 701 g) in the Intra-Spin™ centrifuge (33° rotor angulation, 55 mm radius at the clot, 86 mm at the maximum, Intra-Lock® International, Inc, Boca Raton, FL, USA). In the A-PRF group, the sample was centrifuged at 1500 rpm for 14 minutes (RCF-max = 216 g). After centrifugation, it was possible to observe three different layers: one more superficial, corresponding to the acellular plasma; a lower layer, corresponding to red blood cells; and an intermediate one, corresponding to the PRF matrix. The PRF clot was then collected with specific instruments (Tissue Regeneration Kit and Xpression™ Box, Intra-Lock® International, Inc, Boca Raton, FL, USA) for application in the CSD in their respective groups (Figure 1d).

Creation of CSD

After trichotomy and aseptic preparation, a semilunar incision was made in the scalp in the anterior region of the calvaria, and a full-thickness flap was folded back in the posterior direction (Figure 1a). A 5-mm diameter circular CSD was created in the right parietal bone of each animal with a trephine drill (Neodent®, Curitiba, PR, Brazil) coupled to a low-speed contra-angle under continuous irrigation with sterile saline (Figure 1b). The full-thickness bone segment was gently removed, maintaining the integrity of the dura mater and the encephalon (Figure 1c).

Two circular marks, 2 mm anterior and 2 mm posterior to the margins of the surgical defect, tangent to the longitudinal axis of the CSD, were made with a diamond drill (#1014, KG Sorensen®, Cotia, SP, Brazil) in a high-speed handpiece, under continuous irrigation with sterile saline and aspiration. These marks were filled with amalgam (Amalgam gs-80, SDI Limited, Bayswater, Australia) and will be useful for identifying the site of the original surgical defect during histological laboratory processing.

The surgical defect was left empty in the C group to be filled only with the blood clot. The L-PRF group was filled with L-PRF, and the A-PRF group, with A-PRF. The membranes obtained after compression were divided into two equal parts (Figure 1e). The half closest to the red cells was used to fill the defect, cut into small pieces to better adapt to the surgical site (Figure 1f). The volumes of L-PRF and A-PRF were standardized (0.01 mL) for all animals using an adapted syringe (Figure 1g). After inserting the biomaterial into the CSD (Figure 1h), the other half of the membrane was used to cover the defect and prevent material extravasation (Figure 1i). Then, the soft tissues were repositioned and sutured (Figure 1j) in a simple stitch with 4–0 silk sutures (Ethicon, Johnson & Johnson®, New Jersey, USA).

In the post-operatory, the animals received tramadol hydrochloride (Cronidor 2%, Agener União®, Apucarana, PR, Brazil; 20 mg/kg) and flunixin meglumine (Aplonal 1%, König®, Buenos Aires, Argentina; 2 mg/kg) every 12 hours for two days, intramuscularly.

Characterization of platelet concentrates matrices

An adaptation of Miron et al [33]. was performed to investigate the cells' precise location within L-PRF and A-PRF tubes from rat blood. First, four mL of blood was collected from animals that were not used in the experimental groups of this study in a tube containing ethylenediaminetetraacetic acid solution (EDTA; 5%) as an anticoagulant. Then, 500 µL of this initial sample was pipetted, considered a control (A0).

After centrifugation, following the L-PRF and A-PRF techniques (as described above), sequential layers were pipetted at 350 µL intervals, totalizing ten samples per tube (from the most

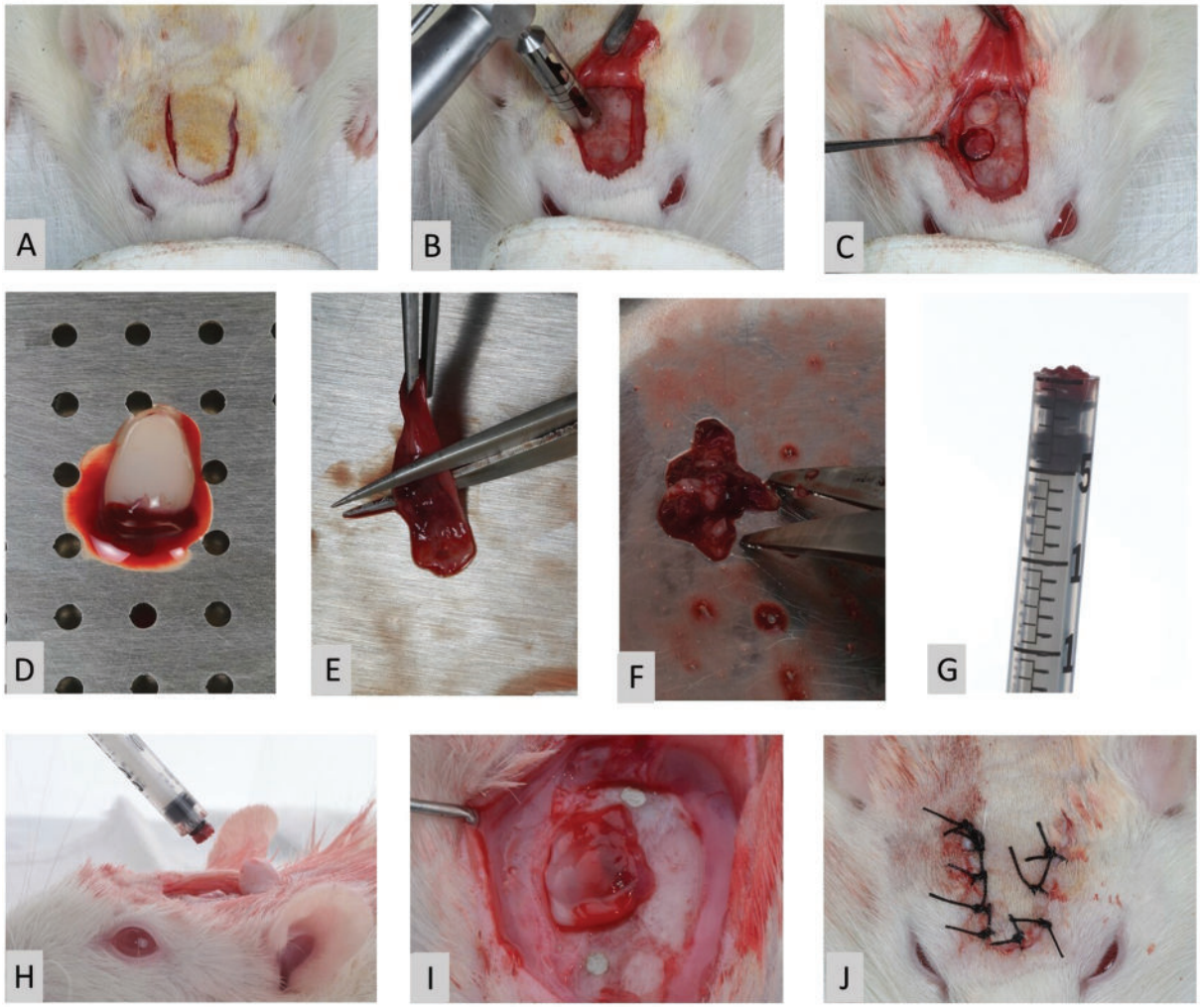

Figure 1. Experimental procedures performed. (a) – Semilunar incision in the animal's calvaria; (b) – Creation of the bone defect with a 5 mm trephine drill; (c) – Bone defect concluded and bone segment being separated; (d) – Platelet concentrate matrix in compressor device; (e) – Section of the platelet concentrate membrane produced; (f) – Portion of the membrane close to the red cell layer being perforated; (g) – Syringe adapted to standardize the volume of platelet concentrate to be used in filling the bone defects; (h) – Standardized volume of platelet concentrate is taken to the bone defect; (i) – Bone defect filled with perforated platelet concentrate and in the form of a membrane; (j) – Suture of the total flap with simple interrupted stitches.

superficial layer to the bottom of the tube - A1/A10). These samples were stored in eppendorf and sent for hematological analysis. First, the number of platelets, leukocytes, and red blood cells in each layer pipetted into each eppendorf was calculated. Notably, one of these samples was collected between the plasma/buffy coat layers and the red cell layer, and this was tagged to represent the location of the buffy coat in the tube.

Euthanasia

All animals were euthanized 35 days after surgery by intramuscular injections of Ketamine 10% (80 mg/kg) and Xylazine 2% (10 mg/kg) for anesthesia, with subsequent completion in a CO_2 chamber with the controlled flow. The area of the original surgical defect and surrounding tissues were removed in blocks and placed in cups with 10% formaldehyde for fixation for 24 hours.

Microtomographic analysis

Nondemineralized specimens of calvaria were scanned by a cone-beam micro-computed tomography (micro-CT) system (SkyScan 1172, Bruker, Kontich, Belgium), generating images in three dimensions (3D). For image acquisition, a spatial resolution of 10 μm was adopted and the x-ray generator operated with an acceleration potential of 60kV, with a current of 165 μA.

Using the DataViewer v.1.4.3 software (SkyScan NV, Kontich, Belgium), the generated 3D image was rotated into a standard position for analysis. Then, a region of interest (ROI) of 5 mm of diameter and a cylindrical volume of interest (VOI) of 0.5x5x5 mm, corresponding to the size of the defect and thickness of the calvaria (0.5 mm), was determined. To assess the trabecular bone tissue in each VOI, a grayscale (0–255) was used, adopting the interval (threshold) between 80 (minimum) and 170 (maximum) to assess the trabecular bone tissue present.

Using the CT-Analyzer® v.1.13.5.1+ software (Bruker, Kontich, Belgium), the following structural parameters were evaluated at each VOI by a calibrated examiner (LMPS): (1) Bone volume (BV) – percentage of VOI filled with bone tissue; (2) Porosity (PO) – percentage of porosity present in the bone tissue determined in the VOI; (3) Number of trabeculae (Tb.N) – number (mm^{-1}) of bone trabeculae present in the VOI; (4) Spacing between trabeculae (Tb.Sp) – total spacing (mm) between bone trabeculae present in the VOI; (5) Thickness of the trabeculae (Tb.Th) – mean thickness (mm) of the bone trabeculae present in the VOI.

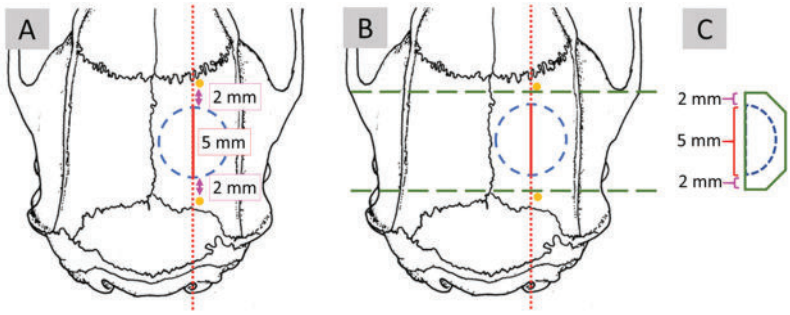

Figure 2. Schematic representation of the reduction of calvaria specimens. (a) – Longitudinal section (dashed line in red) of each specimen in two blocks, precisely along the center of the original surgical defect, using the amalgam marks as a reference. (b) – Cross-section (dashed line in green) tangent to the amalgam marks. (c) - Block with 9 mm of longitudinal extension ready to be embedded in paraffin.

Rendered reconstructions of the microtomographic sections of the calvaria were also obtained.

Histomorphometric analysis

The samples fixed in formalin were rinsed in running water and stored in 70° alcohol. Then, they were decalcified in a 4% EDTA solution. After decalcification, each piece was divided longitudinally into two blocks, precisely along the center of the original surgical defect, using the amalgam marks as a reference (Figure 2a). Cross-sections were made tangent to each of the two amalgam marks (Figure 2b). In this way, it was possible to determine the limits of the surgical defect. Thus, each piece had a size of 9 mm in the longitudinal direction (Figure 2c). After an additional period of decalcification, the samples were then processed and embedded in paraffin. Serial longitudinal four µm-thick sections were performed, starting from the center of the original surgical defect. Two sections of each animal were stained with Hematoxylin and Eosin technique for analysis with light microscopy. In each section, the histopathological characteristics of the neoformed bone tissue were analyzed.

Histometric analysis was performed by a calibrated examiner (D.S.F.S.) using appropriate software (LAS EZ v. 4.1.0, Leica Microsystems® GmbH, Wetzlar, Heidelberg, Germany). One histological section of the central area of the surgical defect of each specimen was selected. Each histological section was photographed using a brightfield fluorescence microscope with a trinocular head (DMLB model, Leica Microsystems® GmbH, Wetzlar, Heidelberg, Germany) with a 1.6x objective lens connected to a camera (DFC300FX, Leica Mycrosystems® GmbH, Wetzlar, Heidelberg, Germany). In each image, a delimitation of the analyzed area was performed, corresponding to the region of the created defect, called Total Area (TA). In addition, the Area of Newly Formed Bone (ANB) was selected and delimited within the TA. The TA value was considered 100% of the analyzed area, and the ANB value was calculated as a percentage of AT (Figure 3).

The histopathological analysis was performed by observing the selected histological sections using the same microscope, with 10x and 20x objective lenses coupled to the same camera used in the histometric study.

Statistical analysis

Statistical analyzes were performed using GraphPad Prism software (v. 5.01, GraphPad Software, Inc, San Diego, CA, USA). The animal was considered the statistical unit. A significance level of 5% ($p < .05$) was adopted for all tests. The Shapiro-Wilk test verified data distribution. The significance of the differences between groups for microtomographic (BV, PO, Tb.N, Tb.Sp, Tb.Th) and histometric (ANB) variables was determined by analysis of variance (ANOVA), followed by Tukey's post hoc test.

Results

Characterization of PRF matrices

The graphs with the number and percentage of leukocytes and platelets are shown in Figure 4. The number of leukocytes (Figure 4a) in the L-PRF was more concentrated in layer 5, representing the buffy coat. Approximately 40% of the leukocytes in the tube were concentrated in this layer (Figure 4c), which had many leukocytes five times greater than that observed in the control sample (A0). Leukocytes were not observed in the first four layers. In A-PRF, leukocytes were more homogeneously distributed throughout the tube, although more concentrated in the buffy coat layer. Compared to the control sample (A0), there was a three times higher concentration of leukocytes in layer five and twice as high in layer 8. No leukocytes were found in the first two layers of the tube.

In L-PRF, platelets were concentrated in layer 5, with an eight-fold increase compared to the control sample (Figure 4b). Thus, approximately 60% of the total platelet in the tube were concentrated in this layer (Figure 4d). Unlike leukocytes, platelets were found throughout the tube, although in very small quantities in the initial four layers and the final four layers. Platelets were found more evenly distributed throughout the tube in A-PRF, although once again concentrated in layers 4 and 5 near the buffy coat zone. In L-PRF, platelets were twice as low in the buffy coat layer (A5) compared to A-PRF.

On the other hand, in A-PRF, there was a 70-fold increase of platelets in the A4 layer compared to L-PRF. Together, the fourth and fifth layers contained 55% of the total platelets in the A-PRF tube. Platelets throughout the tube are significantly greater numbers than the same layers in L-PRF, which indicates a more homogeneous distribution of platelets throughout the tube in A-PRF.

Microtomographic analysis

Figure 5 represents the three-dimensional reconstructions of the calvaria and the graphs of the studied variables.

The L-PRF group (n = 8) presented BV (Mean = 4.960; SD = 1.807), Tb.N (Mean = 0,3190; SD = 0,07758) and Tb.Th (Mean = 0.1375; SD = 0.01610) values significantly higher than those of the C group (n = 8; BV: Mean = 2.096, SD = 1.749; Tb.N: Mean = 0.1445, SD = 0.1270; Tb.Th: Mean = 0.1112, SD = 0.02056; $p < 0,05$). The L-PRF group also presented

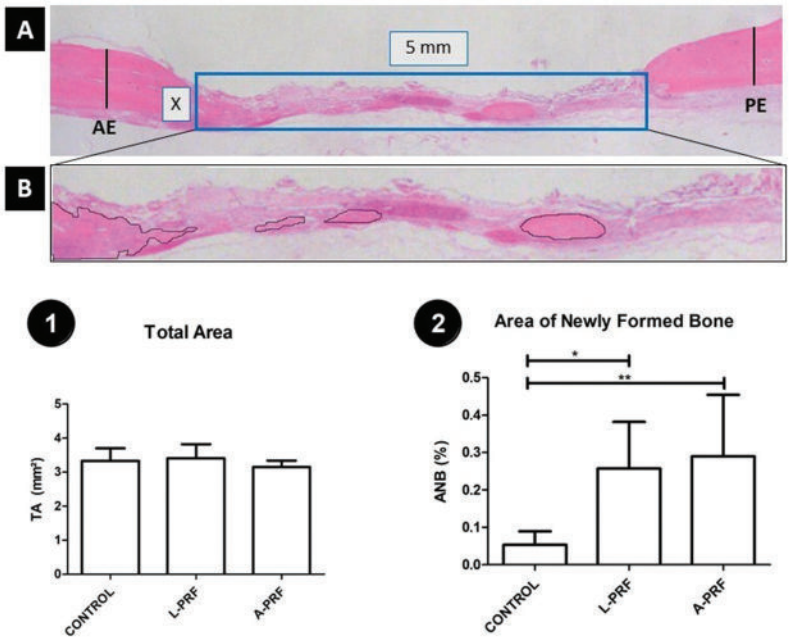

Figure 3. Histometric Analysis. (a) - The Total Area (TA) is delimited by the blue line and corresponds to the area of the calvaria where the surgical defect was created. The simple arithmetic represents TA height (X) mean obtained from the heights of the remaining bone edges anterior (AE) and posterior (PE) to the created defect. The TA width is 5 mm, corresponding to the width of the original defect. Original magnification = 1.6x. (b) - approximation of the TA rectangle represented in A. The Area of Newly Formed Bone (ANB) was calculated as the percentage of neoformed bone (circled in black) to the TA. Means and standard deviations for TA (1) and ANB (2) for C, L-PRF, and A-PRF groups, with the results of the comparisons between groups. Significance value: *p < .05; **p < .01.

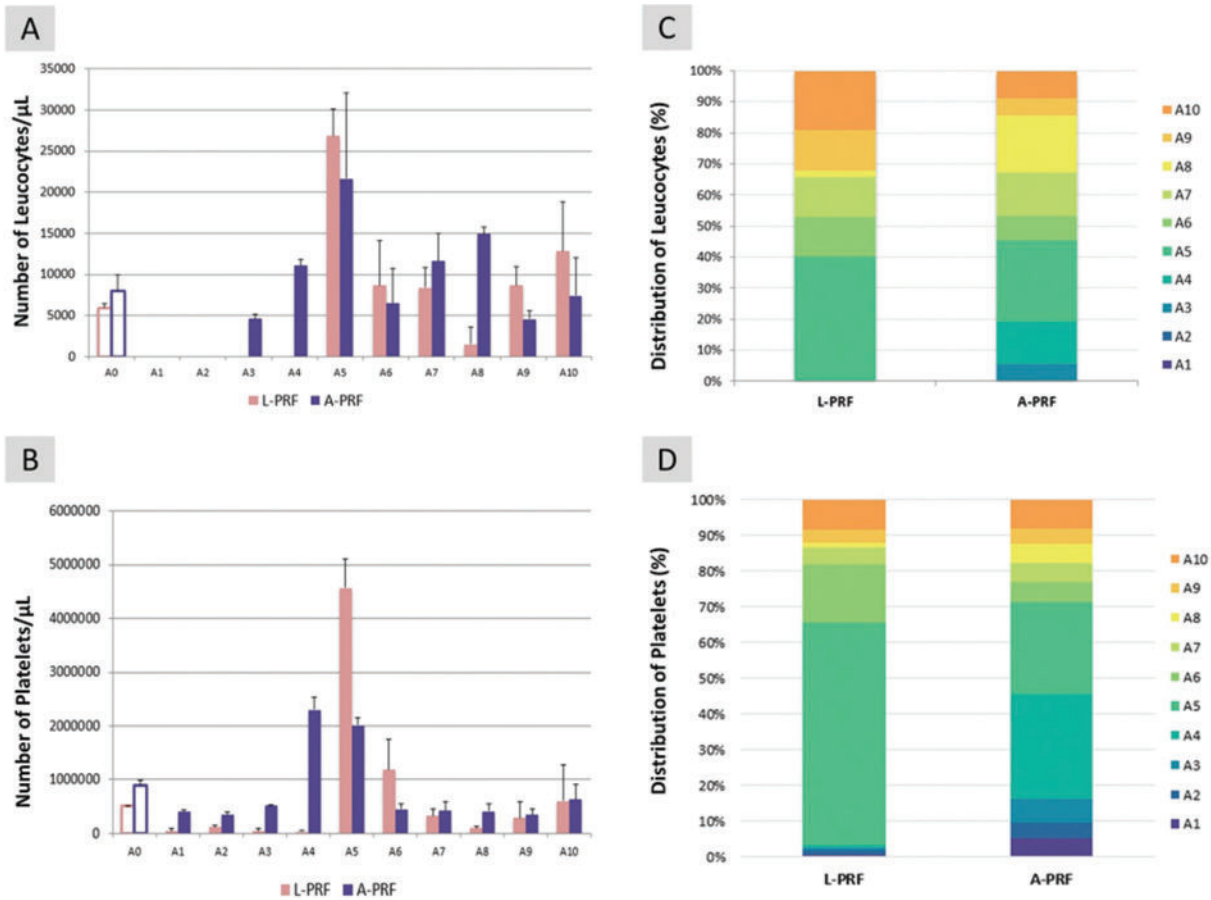

Figure 4. Number of Leukocytes (a) and Platelets (b) in the non-centrifuged blood sample (control sample - A0) and after centrifugation (layers A1 to A10). In (c and d), the percentage distribution of leukocytes and platelets in all layers (A1-A10) after blood centrifugation to prepare L-PRF and A-PRF can be observed. A5 = sample corresponding to the buffy coat layer.

significantly lower PO values (Mean = 95.04, SD = 1.807) than those of the C group (Mean = 97.90, SD = 1.749; p < 0,05). No significant differences were observed between the L-PRF (Mean = 0.5111, SD = 0.007335) and C groups (Mean = 0.5209, SD = 0.008291) for Tb.Sp variable.

The A-PRF group (n = 8) presented BV (Mean = 5.019, SD = 1.401), Tb.N (Mean = 0.3887, SD = 0.09011) and Tb.Th (0.1363, SD = 0.0095) values significantly higher than those of the C group (VO: p < .05; Tb.N: p < 0,01; Tb.Th: p < 0,05), as well as significantly lower values for PO (Mean = 94.98,

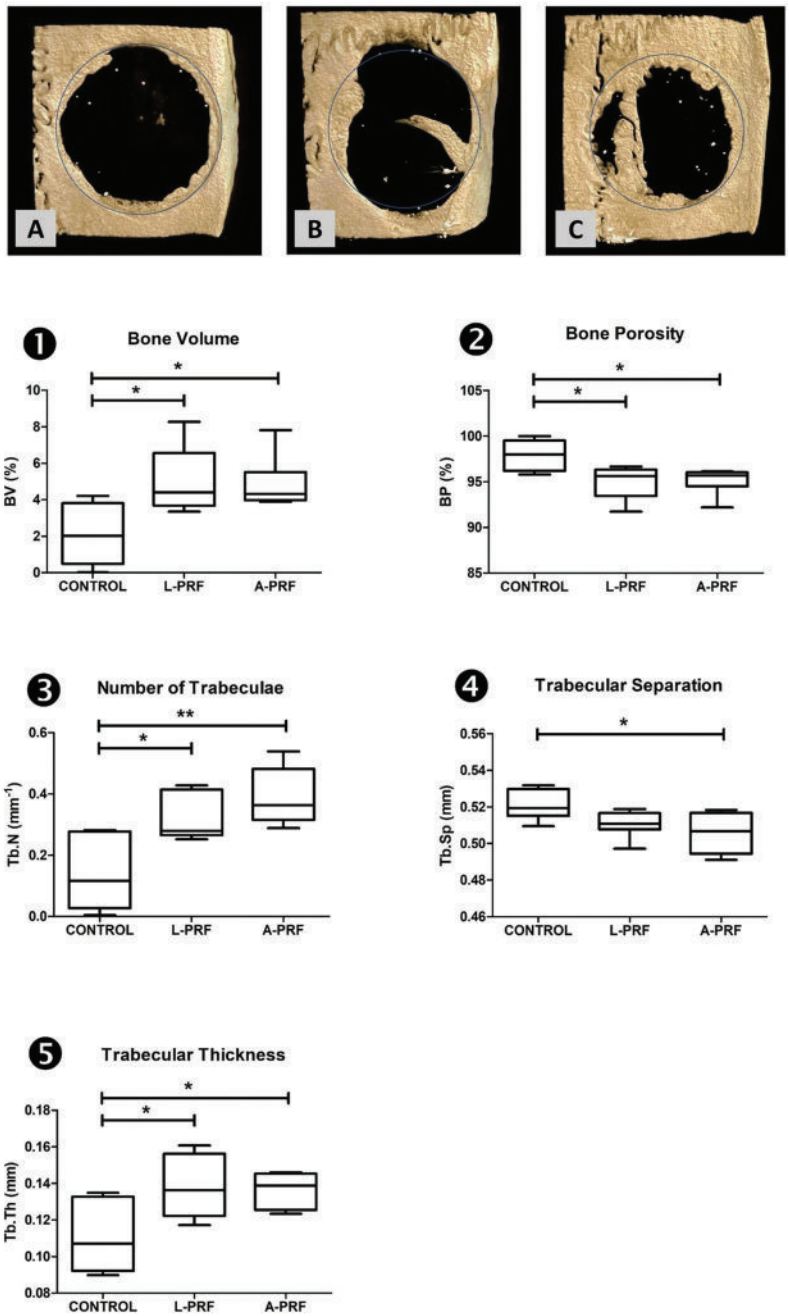

Figure 5. Microtomographic analysis. Rendered reconstructions of the Control (a), L-PRF (b), and A-PRF (c) groups calvaria. Pixel size = 15.9 μm. The blue circle represents the CSD limits. Graphs represented medians, interquartile range, and minimum and maximum values of BV (1), PO (2), Tb.N (3), Tb.Sp (4) and Tb.Th (5) in the microtomographic analysis. ANOVA, Tukey's post hoc test; *p < .05; **p < .01.

SD = 1.401, p < 0,05) and Tb.Sp (Mean = 0.5054, SD = 0.01032, p < 0,05) variables. No significant differences were observed between the A-PRF and L-PRF groups for all microtomographic parameters evaluated (p > 0,05).

Histometric analysis

The L-PRF (n = 8, Mean = 0.2575, SD = 0.1245) and A-PRF (n = 8, Mean = 0.2900, SD = 0.1643) groups presented ANB values significantly higher (p < .05 and p < .01, respectively) than the values of the C group (n = 8; Mean = 0.0533, SD = 0.03615). Although the ANB values were higher in the A-PRF, no significant difference was observed between the L-PRF and A-PRF groups.

Histopathologic analysis

Control group

Almost the entire extent of the surgical defect was filled with connective tissue composed of collagen fibers oriented parallel to the wound surface (Figure 6a). In all specimens, the central part of this connective tissue was much thinner than the original calvaria. In addition, a small amount of neoformed bone tissue was observed along the margins of the surgical defect, showing

a small number of osteoblasts on its edges (Figure 6a,b). The inflammatory infiltrates found throughout the defect were usually mild.

L-PRF group

Most specimens had a greater amount of neoformed bone tissue along the margins of the surgical defect when compared to specimens in the C Group. In some specimens, bone neoformation was observed along with the defect, forming islets (Figure 6c,d) and osteoid matrix zones. The neoformed bone tissue had a small number of osteoblasts at its edges. The connective tissue, without bone differentiation, had numerous bundles of collagen fibers arranged parallel to the wound surface, more organized and thicker than those observed in specimens from the C Group, although still inferior to the thickness of the surgical defect margin. It was observed a significant presence of blood vessels along its entire length.

A-PRF group

Most specimens had a greater amount of neoformed bone tissue near the margins of the surgical defect when compared to specimens from the C and L-PRF groups (Figure 6e,f). The neoformed bone tissue had a small number of osteoblasts at its edges. Some specimens also showed zones of the osteoid matrix along with the defect. The connective tissue, without bone differentiation, presented numerous bundles of collagen fibers parallel to the wound surface but more organized and with greater thickness than those observed in specimens from the C group. A significant presence of blood vessels and the entire extension of the bone defect was observed.

Discussion

The current study is the first to evaluate the bone neoformation of A-PRF in CSD in rats compared to L-PRF. In the present study, both L-PRF and A-PRF proved to be promising therapeutic alternatives in bone regeneration of CSD created in healthy rat calvaria. Furthermore, both potentialized the bone neoformation of surgical defects increased the quality of the formed bone, making it denser.

In the present study, an experimental model capable of guaranteeing a good preparation of L-PRF and A-PRF matrices was used, as well as a test site capable of demonstrating its real potential in bone neoformation. Regarding the blood collection protocol, it is possible to collect up to 15% of the total blood volume of a rat without causing suffering to the animal [34,35]. Considering that the total blood volume of rodents is equivalent to 6 to 8% of its weight and that the average weight of the animals in this investigation was 403 g (data not shown), harvesting 3 mL of blood from the animals was within the acceptable physiological limits. Blood collection in rats can be obtained from several anatomical sites, such as the tail, femoral and jugular veins. This procedure is considered safe for rats and relatively quick to recover [35]. However, these locations do not allow for the collection of a sufficient amount of blood promptly for the PRF technique, since the time between collection and centrifugation must be a maximum of 90 seconds, at the risk of compromising the quality of the membrane [36], and for preventing early clotting in the tube, since this technique does not use anticoagulants [36,37]. The cardiac puncture technique used in the present study enabled the collection of a significant amount of blood at an adequate time. Thus, it was even possible to prepare and evaluate the autogenous membranes of platelet concentrates, similar to the clinical protocol used in humans, since blood from

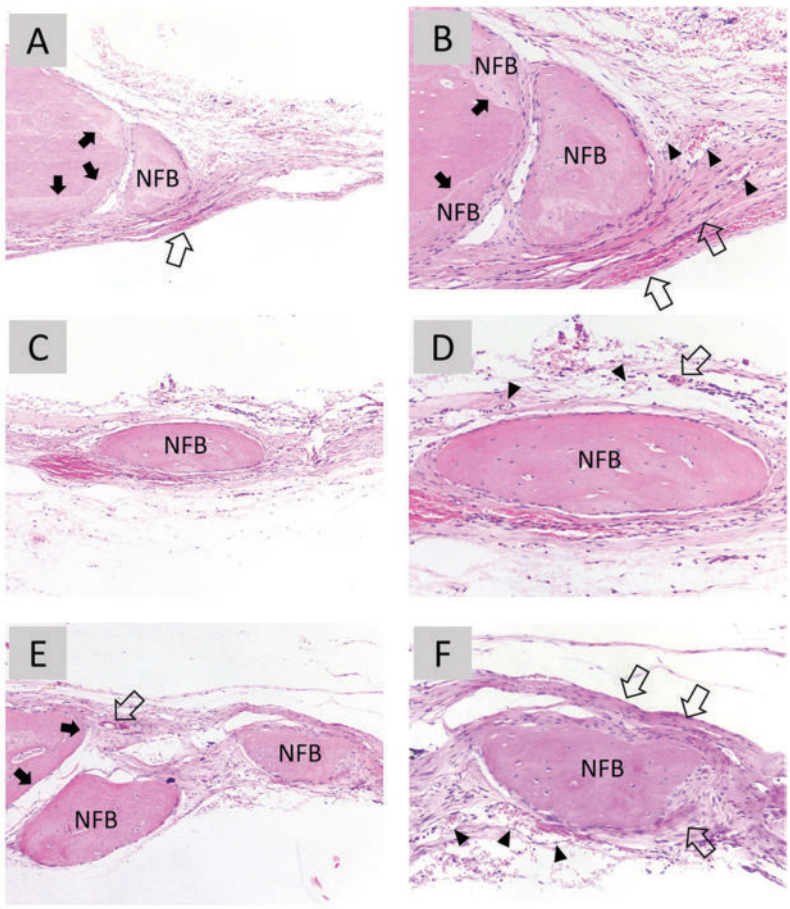

Figure 6. Representative images of histological sections; C (a, b); L-PRF (c, d); A-PRF (e, f) groups. NFB = newly formed bone; arrowhead filled in black color = blood vessels; unfilled arrow = osteoid matrix; arrow filled in black = margins of the original surgical defect; *Images C, D, and F represent distant portions of the surgical defect margins. Coloration: Hematoxicillin and Eosin. Original magnification: 10x (a, c, e); 20x (b, d, f).

animal donors or other animal species could trigger immunological reactions and possible biases in the results obtained [38].

Still considering the experimental model of this study, it is essential to emphasize that the influence of different PRF protocols on bone healing was evaluated in defects deemed to be critical in size. CSD is considered ideal for assessing the impact of material on bone healing, as a complete wound closure is only possible using an osteoconductive, osteogenic, and osteoinductive material[39]. The critical character of the defect was confirmed in this study by the slight bone formation, limited to the margins of the defect, in specimens from the control group. In addition, all specimens showed incomplete wound closure. Since the bone defects of the PRF groups were filled only with PRF and that CSD was used, it can be concluded that the significant increase in bone neoformation observed in the L-PRF and A-PRF groups was due to the biological properties of these biomaterials. However, by definition, PRF is not osteogenic or osteoinductive. Possibly, this increase in bone neoformation occurred due to the immediate presentation of cells necessary for healing, such as platelets and neutrophils, in addition to the supply of natural growth factors that are extremely important in bone regeneration [3,25,37,40]. Previous studies have already demonstrated that using L-PRF can enhance the healing of CSD in healthy rabbit calvaria [41,42], in CSD of healthy rats [43] and osteoporotic rats [31]. It is essential to highlight that the matrix structure of PRF acts as a natural bio skeleton and can decrease the infiltration of fibrous connective tissue. Thus, it is necessary to emphasize that in this study, after filling the CSD of the L-PRF and A-PRF groups with fragmented matrices, intact PRF matrices were placed over the created defects to avoid the displacement of the material placed inside the defect, as no membrane for guided bone regeneration (GBR) was used. It is worth emphasizing that PRF matrices cannot maintain spaces long enough to prevent the invagination of epithelial cells and connective tissue into defects, thus not acting as a natural barrier to GBR due to its rapid degradation [44,45].

In the present study, there was a higher concentration of both leukocytes and platelets in the buffy coat layer of the L-PRF tube. At the same time, there was a greater distribution of these cells along the A-PRF tube, which corroborates the findings from previous studies that characterized PRF matrices produced according to the low centrifugation protocol [27,33,46]. Thus, in this study, the L-PRF and A-PRF matrices presented different amounts and distributions of cells, following the patterns observed in matrices produced with these protocols from human blood. It is important to consider that platelet and leukocyte counts were performed on anticoagulated blood samples. The distribution of these cells in the PRF samples produced without anticoagulants and used in the animals of the experimental groups of this study may present some variations in these cell counts. Although the levels of growth factors present in both matrices have not been evaluated, it can be deduced that differences between them may have occurred since there is a relationship between the number of cells present in the platelet concentrates and the levels of growth factors [29,41]. Furthermore, it has been shown that low-speed centrifugation protocols favor an increase in the release of growth factors in PRF clots compared to high-speed centrifugation protocols [29,47]. Unlike these results, Dohan et al [48]. observed that the slow release of some growth factors from original L-PRF membranes was significantly more potent at all experimental times than the release from A-PRF membranes. Future studies are essential to finding a correlation between the number of growth factors present in both matrices and the amount of newly formed bone stimulated by them.

This proof-of-concept study did not demonstrate significant differences in the amount of bone neoformation between the L-PRF and A-PRF groups (BV and ANB analyses). Although the potential of platelet concentrates in the bone neoformation process has been quite evident (defects treated with both matrices had higher BV and ANB when compared to control defects), variations in the production protocols of PRF matrices do not seem to have impacted the biological results. Several advantages arising from reduced centrifugation speed for the preparation of PRF matrices have been highlighted in several *in vitro* studies [26,27,29,47]. Only one *in vivo* study compared the regenerative potential of PRF matrices produced in high and low-speed centrifugation protocols from their implantation in subcutaneous tissues of rats [30]. The results of this study [30] demonstrated that PRF matrices produced with high centrifugation protocols had a dense and stable fibrin structure that prevented host tissue penetration. On the other hand, the PRF made in a low-speed centrifugation protocol was more porous and presented a higher vascularization rate when implanted in the subcutaneous tissue of rats. These findings highlighted the possibility of altering the regenerative potential of PRF matrices by modifying their structure and composition.

The present study is the first to compare the potential of PRF matrices produced through high- and low-speed centrifugation protocols in bone neoformation. Although no significant differences were observed in the amount of bone neoformation between the L-PRF and A-PRF groups, it is important to emphasize some aspects observed in the qualitative histological analysis and the analysis of bone microarchitecture of the experimental groups. Compared to defects treated with L-PRF, defects treated with A-PRF had a more significant amount of osteoid matrix and a smaller spacing between bone trabeculae. Studies with longer follow-up times and immunohistochemical analyses would better explain the results obtained and highlight the possible molecular impacts arising from changes in the composition of PRF matrices.

It is essential to consider that, in the present study, the PRF matrices were used alone, unlike the various clinical situations in which it is associated with bone grafts and biomaterials [41,43,49,50]. Engler-Pinto et al [31]. demonstrated less bone volume in defects filled with L-PRF alone than in defects filled only with xenogenous bone graft. The authors argued that this result could be explained considering the rate of degradation of L-PRF clots. While the L-PRF clot can be rapidly degraded, Bio-Oss® particles exhibit slow resorption. They can act as a scaffold for cell migration and new blood vessel formation, which is crucial for predictable and efficient bone regeneration [43]. Thus, further studies comparing A-PRF and L-PRF matrices associated with bone grafts and biomaterials are important.

The main limitation of this study is the absence of analysis to quantify the levels of growth factors in the different PRF matrices to establish a correlation with the amount of newly formed bone in each experimental group. Future studies are essential to address this topic. Furthermore, tests on animals of a larger phylogenetic scale should also be performed, as well as on animals with systemic impairments and more extended follow-up periods. Finally, an immunohistochemical analysis may be necessary for conclusions regarding the rate of bone neoformation and the future potential of present tissues for neoformed bone.

Conclusion

Within the limits of this study, it can be concluded that i) platelet concentrates produced with high and low centrifugation speeds potentiated the healing of CSD in rat calvaria; ii) high and low-speed centrifugation protocols did not produce PRF matrices with different biological impacts on the amount of bone neoformation.

Acknowledgements

The authors would like to thank the Coordination for the Improvement of Higher Education Personnel (CAPES - process #00.889.834/0001-08; scholarship for L.M.P.S.)

Disclosure statement

No potential conflict of interest was reported by the author(s).

Funding

The author(s) reported there is no funding associated with the work featured in this article.

ORCID

Lucia Moitrel Pequeno da Silva http://orcid.org/0000-0003-3317-8393
Débora de Souza Ferreira Sávio http://orcid.org/0000-0003-4073-0297
Felipe Correa de Ávila http://orcid.org/0000-0002-3628-2578
Raphael Martini Vicente http://orcid.org/0000-0001-6454-8014
Gabriel Guerra David Reis http://orcid.org/0000-0002-9541-5238
Ricardo Junior Denardi http://orcid.org/0000-0001-8312-7493
Natacha Malu Miranda da Costa http://orcid.org/0000-0001-7852-4697
Pedro Henrique Felix Silva http://orcid.org/0000-0002-7583-7046
Carlos Fernando de Almeida Barros Mourão http://orcid.org/0000-0001-5775-0222
Richard J. Miron http://orcid.org/0000-0003-3290-3418
Michel Reis Messora http://orcid.org/0000-0001-8485-9645

References

1. Choukroun J, Adda F, Schoeffler C, Vervelle A. Une opportunité en paro-implantologie: le PRF. Implantodontie 2001;42:55–62.
2. Choukroun J, Diss A, Simonpieri A, Girard M-O, Schoeffler C, Dohan SL, Dohan AJJ, Mouhyi J, Dohan DM. Platelet-rich fibrin (PRF): a second-generation platelet concentrate. Part V: histologic evaluations of PRF effects on bone allograft maturation in sinus lift. Oral Surg Oral Med Oral Pathol Oral Radiol Endodontol 2006;101:299–303. doi:10.1016/j.tripleo.2005.07.012.
3. Choukroun J, Diss A, Simonpieri A, Girard M-O, Schoeffler C, Dohan SL, Dohan AJJ, Mouhyi J, Dohan DM. Platelet-rich fibrin (PRF): a second-generation platelet concentrate. Part IV: clinical effects on tissue healing. Oral Surg Oral Med Oral Pathol Oral Radiol Endodontol 2006;101:e56–e60. doi:10.1016/j.tripleo.2005.07.011.
4. Alzahrani AA, Murriky A, Shafik S. Influence of platelet rich fibrin on post-extraction socket healing: a clinical and radiographic study. Saudi Dental J 2017;29:149–155. doi:10.1016/j.sdentj.2017.07.003.
5. Hauser F, Gaydarov N, Badoud I, Vazquez L, Bernard J-P, Ammann P. Clinical and histological evaluation of post-extraction platelet-rich fibrin socket filling: a prospective randomized controlled study. Bone 2012;50:S113. doi:10.1016/j.bone.2012.02.348.
6. Kumar N, Prasad K, Ramanujam L, Ranganath K, Dexith J, Chauhan A. Evaluation of treatment outcome after impacted mandibular third molar surgery with the use of autologous platelet-rich fibrin: a randomized controlled clinical study. J Oral Maxillofacial Surg 2015;73:1042–1049. doi:10.1016/j.joms.2014.11.013.
7. Mourão CFAB, de Mello-Machado RC, Javid K, Moraschini V. The use of leukocyte- and platelet-rich fibrin in the management of soft tissue healing and pain in post-extraction sockets: a randomized clinical trial. J Cranio-Maxillofacial Surg 2020;48:452–457. doi:10.1016/j.jcms.2020.02.020.
8. Temmerman A, Vandessel J, Castro A, Jacobs R, Teughels W, Pinto N, Quirynen M. The use of leucocyte and platelet-rich fibrin in socket management and ridge preservation: a split-mouth, randomized, controlled clinical trial. J Clin Periodontol 2016;43:990–999. doi:10.1111/jcpe.12612.
9. Hiremath H, Motiwala T, Jain P, Kulkarni S. Use of second-generation platelet concentrate (platelet-rich fibrin) and hydroxyapatite in the management of large periapical inflammatory lesion: a computed tomography scan analysis. Indian J Dent Res 2014;25:517. doi:10.4103/0970-9290.142556.
10. Jayalakshmi KB, Agarwal S, Singh MP, Vishwanath BT, Krishna A, Agrawal R. Platelet-rich fibrin with β-tricalcium phosphate — a noval approach for bone augmentation in chronic periapical lesion: a case report. Case Rep Dent 2012;2012:1–6. doi:10.1155/2012/902858.
11. Johns D, Vidyanath S, Sam G, Shivashankar V. Combination of platelet rich fibrin, hydroxyapatite and PRF membrane in the management of large inflammatory periapical lesion. J Conserv Dent 2013;16:261. doi:10.4103/0972-0707.111329.
12. Ali S, Bakry SA, Abd-Elhakam H. Platelet-rich fibrin in maxillary sinus augmentation: a systematic review. J Oral Implantol 2015;41:746–753. doi:10.1563/AAID-JOI-D-14-00167.
13. Kanayama T, Horii K, Senga Y, Shibuya Y. Crestal approach to sinus floor Elevation for atrophic maxilla using platelet-rich fibrin as the only grafting material: a 1-year prospective study. Implant Dent 2016;25:32–38. doi:10.1097/ID.0000000000000327.
14. Mazor Z, Horowitz RA, Del Corso M, Prasad HS, Rohrer MD, Dohan Ehrenfest DM. Sinus floor augmentation with simultaneous implant placement using Choukroun's platelet-rich fibrin as the sole grafting material: a radiologic and Histologic study at 6 months. J Periodontol 2009;80:2056–2064. doi:10.1902/jop.2009.090252.
15. Simonpieri A, Choukroun J, Corso MD, Sammartino G, Ehrenfest DMD. Simultaneous sinus-lift and implantation using microthreaded implants and leukocyte- and platelet-rich fibrin as sole grafting material: a six-year experience. Implant Dent 2011;20:2–12. doi:10.1097/ID.0b013e3181faa8af.
16. Tatullo M, Marrelli M, Cassetta M, Pacifici A, Stefanelli LV, Scacco S, Dipalma G, Pacifici L, Inchingolo F. Platelet Rich Fibrin (P.R.F.) in reconstructive surgery of atrophied maxillary bones: clinical and histological evaluations. Int J Med Sci 2012;9:872–880. doi:10.7150/ijms.5119.
17. Zhang Y, Tangl S, Huber CD, Lin Y, Qiu L, Rausch-Fan X. Effects of Choukroun's platelet-rich fibrin on bone regeneration in combination with deproteinized bovine bone mineral in maxillary sinus augmentation: a histological and histomorphometric study. J Cranio-Maxillofacial Surg 2012;40:321–328. doi:10.1016/j.jcms.2011.04.020.
18. Eren G, Atilla G. Platelet-rich fibrin in the treatment of localized gingival recessions: a split-mouth randomized clinical trial. Clin Oral Invest 2014;18:1941–1948. doi:10.1007/s00784-013-1170-5.
19. Öncü E. The use of platelet-rich fibrin versus subepithelial connective tissue graft in treatment of multiple gingival recessions: a randomized clinical trial. Int J Periodontics Restorative Dent 2017;37:265–271. doi:10.11607/prd.2741.
20. Tunali M, Ozdemir H, Arabaci T, Gurbuzer B, Pikdoken L, Firatli E. Clinical evaluation of autologous platelet-rich fibrin in the treatment of multiple adjacent gingival recession defects: a 12-month study. Int J Periodontics Restorative Dent 2015;35:105–114. doi:10.11607/prd.1826.
21. Panda S, Doraiswamy J, Malaiappan S, Varghese SS, Del Fabbro M. Additive effect of autologous platelet concentrates in treatment of intrabony defects: a systematic review and meta-analysis. J Invest Clin Dent 2016;7:13–26. doi:10.1111/jicd.12117.
22. Sharma A, Pradeep AR. Treatment of 3-wall intrabony defects in patients with chronic periodontitis with autologous platelet-rich fibrin: a randomized controlled clinical trial. J Periodontol 2011;82:1705–1712. doi:10.1902/jop.2011.110075.
23. Asaka T, Ohga N, Yamazaki Y, Sato J, Satoh C, Kitagawa Y. Platelet-rich fibrin may reduce the risk of delayed recovery in tooth-extracted patients undergoing oral bisphosphonate therapy: a trial study. Clin Oral Invest 2017;21:2165–2172. doi:10.1007/s00784-016-2004-z.
24. Cano-Duran J, Pena-Cardelles J, Ortega-Concepcion D, Paredes-Rodriguez V, Garcia-Riart M, Lopez-Quiles J. The role of Leucocyte-rich and platelet-rich fibrin (L-PRF) in the treatment of the medication-related osteonecrosis of the jaws (MRONJ). J Clin Exp Dent 2017. doi:10.4317/jced.54154.
25. Dohan DM, Choukroun J, Diss A, Dohan SL, Dohan AJJ, Mouhyi J, Gogly B. Platelet-rich fibrin (PRF): a second-generation platelet

concentrate. Part I: technological concepts and evolution. Oral Surg Oral Med Oral Pathol Oral Radiol Endodontol 2006;101:e37–e44. doi:10.1016/j.tripleo.2005.07.008.
26. Ghanaati S, Booms P, Orlowska A, Kubesch A, Lorenz J, Rutkowski J, Landes C, Sader R, Kirkpatrick C, Choukroun J. Advanced platelet-rich fibrin: a new concept for cell-based tissue engineering by means of inflammatory cells. J Oral Implantol 2014;40:679–689. doi:10.1563/aaid-joi-D-14-00138.
27. El Bagdadi K, Kubesch A, Yu X, Al-Maawi S, Orlowska A, Dias A, Booms P, Dohle E, Sader R, Kirkpatrick CJ, et al. Reduction of relative centrifugal forces increases growth factor release within solid platelet-rich-fibrin (PRF)-based matrices: a proof of concept of LSCC (low speed centrifugation concept). Eur J Trauma Emerg Surg 2019;45:467–479. doi:10.1007/s00068-017-0785-7.
28. Miron RJ, Xu H, Chai J, Wang J, Zheng S, Feng M, Zhang X, Wei Y, Chen Y, de Mourão CFAB, et al. Comparison of platelet-rich fibrin (PRF) produced using 3 commercially available centrifuges at both high (~ 700 g) and low (~ 200 g) relative centrifugation forces. Clin Oral Invest 2020;24:1171–1182. doi:10.1007/s00784-019-02981-2.
29. Fujioka-Kobayashi M, Miron RJ, Hernandez M, Kandalam U, Zhang Y, Choukroun J. Optimized platelet-rich fibrin with the low-speed concept: growth factor release, biocompatibility, and cellular response. J Periodontol 2017;88:112–121. doi:10.1902/jop.2016.160443.
30. Kubesch A, Barbeck M, Al-Maawi S, Orlowska A, Booms PF, Sader RA, Miron RJ, Kirkpatrick C, Choukroun J, Ghanaati S. A low-speed centrifugation concept leads to cell accumulation and vascularization of solid platelet-rich fibrin: an experimental study *in vivo*. Platelets 2019;30:329–340. doi:10.1080/09537104.2018.1445835.
31. Engler-Pinto A, Siéssere S, Calefi A, Oliveira L, Ervolino E, Souza S, Furlaneto F, Messora MR. Effects of leukocyte- and platelet-rich fibrin associated or not with bovine bone graft on the healing of bone defects in rats with osteoporosis induced by ovariectomy. Clin Oral Impl Res 2019;30:962–976. doi:10.1111/clr.13503.
32. Nagata MJ, Messora M, Pola N, Campos N, Vieira R, Esper LA, Sbrana M, Fucini S, Garcia V, Bosco A. Influence of the ratio of particulate autogenous bone graft/platelet-rich plasma on bone healing in critical-size defects: a histologic and histometric study in rat calvaria. J Orthop Res 2010;28:468–473. doi:10.1002/jor.21027.
33. Miron RJ, Chai J, Zheng S, Feng M, Sculean A, Zhang Y. A novel method for evaluating and quantifying cell types in platelet rich fibrin and an introduction to horizontal centrifugation. J Biomed Mater Res 2019;107:2257–2271. doi:10.1002/jbm.a.36734.
34. Harkness JE, Wagner JE. Clinical procedures. The biology and medicine of rabbits and rodents. Philadelphia, PA: Williams & Wilkings; 2010. p. 107–194.
35. Hoff J. Methods of blood collection in the mouse. Lab Anim (NY) 2000;29:47–53.
36. Miron RJ, Dham A, Dham U, Zhang Y, Pikos MA, Sculean A. The effect of age, gender, and time between blood draw and start of centrifugation on the size outcomes of platelet-rich fibrin (PRF) membranes. Clin Oral Invest 2019;23:2179–2185. doi:10.1007/s00784-018-2673-x.
37. Dohan Ehrenfest DM, Del Corso M, Diss A, Mouhyi J, Charrier J-B. Three-dimensional architecture and cell composition of a Choukroun's platelet-rich fibrin clot and membrane. J Periodontol 2010;81:546–555. doi:10.1902/jop.2009.090531.
38. Ghanaati S, Al-Maawi S, Herrera-Vizcaino C, Alves GG, Calasans-Maia MD, Sader R, Kirkpatrick CJ, Choukroun J, Bonig H, Cfab DM. A proof of the low speed centrifugation concept in rodents: new perspectives for *In Vivo* research. Tissue Eng Part C Methods 2018;24:659–670. doi:10.1089/ten.tec.2018.0236.
39. Bosch C, Melsen B, Vangervik K. Importance of the critical-size bone defect in testing bone-regenerating materials. J Craniofac Surg 1998;9:310–316. doi:10.1097/00001665-199807000-00004.
40. Kang Y-H, Jeon SH, Park J-Y, Chung J-H, Choung Y-H, Choung H-W, Kim E-S, Choung P-H. Platelet-rich fibrin is a bioscaffold and reservoir of growth factors for tissue regeneration. Tissue Eng Part A 2011;17:349–359. doi:10.1089/ten.TEA.2010.0327.
41. Acar AH, Yolcu Ü, Gül M, Keleş A, Erdem NF, Altundag Kahraman S. Micro-computed tomography and histomorphometric analysis of the effects of platelet-rich fibrin on bone regeneration in the rabbit calvarium. Arch Oral Biol 2015;60:606–614. doi:10.1016/j.archoralbio.2014.09.017.
42. Pripatnanont P, Nuntanaranont T, Vongvatcharanon S, Phurisat K. The primacy of platelet-rich fibrin on bone regeneration of various grafts in rabbit's calvarial defects. J Cranio-Maxillofacial Surg 2013;41:e191–e200. doi:10.1016/j.jcms.2013.01.018.
43. Sindel A, Dereci Ö, Toru HS, Tozoğlu S. Histomorphometric comparison of bone regeneration in critical-sized bone defects using demineralized bone matrix, platelet-rich fibrin, and hyaluronic acid as bone substitutes. J Craniofacial Surg 2017;28:1865–1868. doi:10.1097/SCS.0000000000003588.
44. Isobe K, Watanebe T, Kawabata H, Kitamura Y, Okudera T, Okudera H, Uematsu K, Okuda K, Nakata K, Tanaka T, et al. Mechanical and degradation properties of advanced platelet-rich fibrin (A-PRF), concentrated growth factors (CGF), and platelet-poor plasma-derived fibrin (PPTF). Int J Implant Dent 2017;3:17. doi:10.1186/s40729-017-0081-7.
45. Kawase T, Kamiya M, Kobayashi M, Tanaka T, Okuda K, Wolff L, Yoshie H. The heat-compression technique for the conversion of platelet-rich fibrin preparation to a barrier membrane with a reduced rate of biodegradation. J Biomed Mater Res B Appl Biomater 2015;103:825–831. doi:10.1002/jbm.b.33262.
46. Sato A, Kawabata H, Aizawa H, Tsujino T, Isobe K, Watanabe T, Kitamura Y, Miron RJ, Kawase T. Distribution and quantification of activated platelets in platelet-rich fibrin matrices. Platelets 2020:1–6. doi:10.1080/09537104.2020.1856359.
47. Kobayashi E, Flückiger L, Fujioka-Kobayashi M, Sawada K, Sculean A, Schaller B, Miron RJ. Comparative release of growth factors from PRP, PRF, and advanced-PRF. Clin Oral Invest 2016;20:2353–2360. doi:10.1007/s00784-016-1719-1.
48. Dohan Ehrenfest DM, Pinto NR, Pereda A, Jiménez P, Del Corso M, Kang B, Nally M, Lanata N, Wang H, Quirynen M. The impact of the centrifuge characteristics and centrifugation protocols on the cells, growth factors, and fibrin architecture of a leukocyte- and platelet-rich fibrin (L-PRF) clot and membrane. Platelets 2018;29:171–184. doi:10.1080/09537104.2017.1293812.
49. Oliveira MR, deC. Silva A, Ferreira S, Avelino CC, Garcia IR, Mariano RC. Influence of the association between platelet-rich fibrin and bovine bone on bone regeneration. A histomorphometric study in the calvaria of rats. Int J Oral Maxillofac Surg 2015;44:649–655. doi:10.1016/j.ijom.2014.12.005.
50. Clark D, Rajendran Y, Paydar S, Ho S, Cox D, Ryder M, Dollard J, Kao RT. Advanced platelet-rich fibrin and freeze-dried bone allograft for ridge preservation: a randomized controlled clinical trial. J Periodontol 2018;89:379–387. doi:10.1002/JPER.17-0466.